

REMARKS

Claim 1 calls for a semiconductor structure and a removable material on the semiconductor structure. A curved microspring is formed over said removable material. A spring arm is formed on the semiconductor structure over the microspring. The cited reference to Bishop is asserted to teach a semiconductor structure 26. It is argued that a removable material is removed from layers 12 and 26. But even if this were so, it is not pertinent to the claim since the claim requires the removable material to be under the microspring. This is because the claim calls for a curved microspring formed over the removable material. The cited reference to Bishop does not teach a microspring as apparently conceded and, therefore, it most certainly does not teach a microspring formed over a removable material. Thus, Bishop fails to meet the claim limitations.

Sobhani does not cure the deficiencies inherent in Bishop. While the office action is silent on how Sobhani is applied, presumably, the Examiner relies on the dimple 18. But there is nothing to suggest that the dimple 18 is a microspring or that it is formed over removable material. Therefore, the pertinency of Sobhani is not understood.


Even if there were some rationale to combine the two references, which there most certainly is not, there still is no teaching of a curved microspring formed over a removable material. A microspring is a term of art in the microelectromechanical systems (MEMS) field. It refers to a spring on the order of integrated circuit size. Plainly, the claim refers to such a device since it calls for a microspring to be formed on a semiconductor structure. Attached are a number of publications from the MEMS field which refer to MEMS microsprings in this way. In addition, neither reference nor their combination teaches forming a microspring over a semiconductor structure as claimed. The fact that someone used a large spring does not teach that it would be obvious to make a similar type of structure on an integrated circuit scale.

Claim 22 further calls for the removable material to a material that is removable through the application of heat. Claim 22 defines the type of material. The claimed material is one that is removable through the application of heat. The assertion that the method of heating is not germane to the issue of patentability of the product itself is true, but provides no basis to reject the claim. The refusal to give patentable weight to the material limitation should be reconsidered.

In view of these remarks, reconsideration is requested.

Respectfully submitted,

Date: August 17, 2004



Timothy N. Trop, Reg. No. 28,994
TROP, PRUNER & HU, P.C.
8554 Katy Freeway, Ste. 100
Houston, TX 77024
713/468-8880 [Phone]
713/468-8883 [Fax]



SINGLE CRYSTAL SILICON AS A MICROMECHANICAL MATERIAL

H. Kahn^{*}, M.J. Troyer², V.R. Prabhu², C.-L. Shih¹, S.M. Phillips², M.A. Huff², and A.H. Heuer^{*}

¹Department of Materials Science and Engineering, ²Department of Electrical Engineering and Applied Physics, Case Western Reserve University, 10900 Euclid Ave., Cleveland, Ohio 44106 ^{*}kahn@mems3.cwru.edu

ABSTRACT

Single crystal silicon is the standard substrate for both bulk- and surface-micromachined microelectromechanical systems (MEMS). However, it can also be used as a structural material itself in microdevices. In particular, single crystal silicon micro-springs have been designed and fabricated. These springs, which are approximately 20 μm thick and 7 mm across, incorporate a central island that can be used to apply force to an external device, such as a microvalve or micropump. Varying designs can exhibit deflections of 50 to 1500 μm under applied loads of 5 to 50 mN. The spring behavior has been fully characterized by mechanical testing and by finite element analysis. The micromachining techniques used to fabricate these devices create distinct surfaces of varying morphology, depending on the etching methods used. The fracture behavior of these diverse silicon surfaces is examined to ensure and improve the reliability of the devices.

INTRODUCTION

Silicon-based bulk-micromachined microvalves which use TiNi shape memory alloy thin films as actuators have been previously fabricated and reported.¹

These valves were capable of modulating water flow rates up to 5 ml/min, and utilized an external biasing spring acting in opposition to the shape memory effect of the actuator in order to achieve the opening and closing of the valve. However, it is the goal of all MEMS devices to be bulk manufacturable for cost considerations. As a result, an integrated spring, based on the same silicon micromachining techniques as the valve, is highly desirable. One candidate for this application is a planar microspring etched from a single crystal silicon wafer. This spring can then be bonded to the actuator and orifice wafers which comprise the remainder of the microvalve. A schematic cross-sectional drawing of this microvalve configuration is shown in Figure 1.

The forces generated by the TiNi actuator in the microvalve establish the parameters which must be adhered to by the spring design. Specifically, a restoring force of 0.1 N for an out-of-plane deflection of 150 μm is required to close the valve. During opening of the microvalve, the spring must deflect an additional 250 μm . The planar microspring is confined to a square area with a width of 7 mm; in addition, a 3 mm wide square of silicon must remain in the center in order to apply the bias force, as seen in Figure 1.

To the extent authorized under the laws of the United States of America, all copyright interests in this publication are the property of The American Ceramic Society. Any duplication, reproduction, or republication of this publication or any part thereof without the express written consent of The American Ceramic Society or fee paid to the Copyright Clearance Center, is prohibited.

Reprinted from Ceramic Transactions, Vol 66, 1998
Copyright © 1998 by The American Ceramic Society

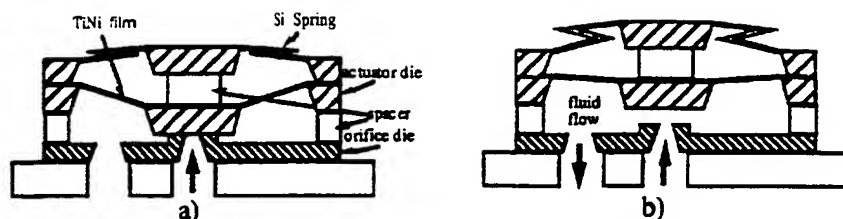


Figure 1. Schematic cross-sections of a micromachined valve, using an integrated silicon spring - in a) the valve is in the cold/closed state; in b) the valve is in the heated/open state.

PROCEDURE

The planar silicon microsprings were fabricated using standard micromachining techniques. The processing sequence is sketched in Figure 2, and is summarized, as follows. Four inch diameter, 525 μm thick single crystal (100) wafers are oxidized to a thickness of 1.5 μm . Photolithography is used to pattern the oxide on the backside of the wafers to define the square areas to be used as the springs, and the oxide is etched in hydrofluoric acid (Figure 2a). The silicon wafers are etched in potassium hydroxide (KOH), which is an anisotropic silicon etch that etches much more quickly in the [100] than in the [111] directions, to create silicon diaphragms of $\sim 10\text{-}30\ \mu\text{m}$ thickness (Figure 2b). The oxide on the front side of the wafers is photolithographically patterned and chemically etched to define the shape of the springs (Figure 2c). The $\sim 30\ \mu\text{m}$ of silicon is reactive ion etched in an SF_6 ambient, and the remaining oxide is chemically removed. This forms the $\sim 10\text{-}30\ \mu\text{m}$ thick silicon spring, supported by a 525 μm thick frame, attached to a central 525 μm thick square island (Figure 2d). These standard processing techniques, in particular the reactive ion etching, limit the thickness of the silicon microspring to a maximum of $\sim 30\ \mu\text{m}$.

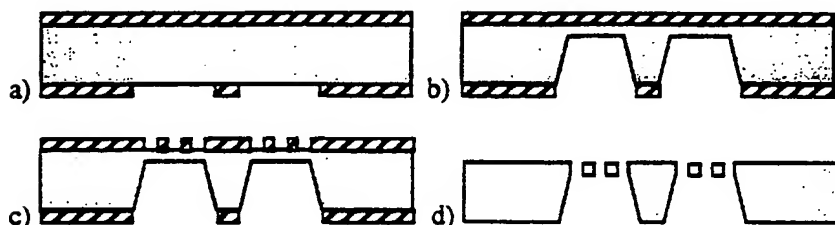


Figure 2. Microspring fabrication procedure. See text for further details

Finite element analysis (FEA) was extensively used to characterize the structural properties of the silicon spring while in use. This technique can predict the displacement of the spring under varying loads, taking into account bending, torsion, and shear, in an efficient manner which would be impossible by analytical methods. It is used to model the deflection of the microspring under varying loads, and thus to determine the optimum spring design for the present application.

Besides providing the appropriate restoring force to the valve, the microspring must also be robust enough to survive the required displacements without fracturing. As seen in the processing sequence described in Figure 2, the springs will have two distinct surface. The top surface is created by the oxidation of the polished silicon wafer and subsequent chemical removal of the oxide, and the bottom surface is created by KOH etching. As shown in the micrographs in Figure 3, the two surface morphologies are quite different. Single crystal silicon bend bars were fabricated in a manner similar to that described in Figure 2 - specifically, the top and bottom surfaces of the bend bars were created in the same way as for the springs. The bend bars were then subjected to four point bending. Various specimens were tested with either surface in tension to determine the fracture behaviors.

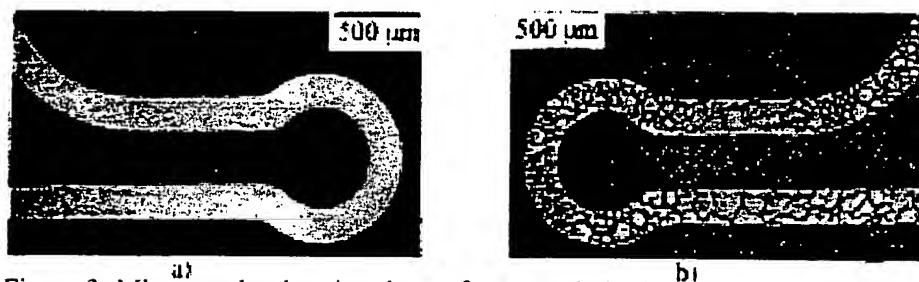


Figure 3. Micrographs showing the surface morphologies of a) polished silicon and b) KOH etched silicon.

RESULTS AND DISCUSSION

The results for the four point bending tests on the single crystal silicon bend bars are shown in the Weibull plot in Figure 4. The KOH etched surface exhibits a greater fracture resistance. This is presumably due to the removal of some of the sharpest surface defects during the etch. Unfortunately, the current design of the microvalve assembly puts the polished silicon surface in tension during valve operation. This could be corrected by an appropriate adjustment of the processing sequence, but for the present spring designs a further requirement will be a maximum strain of 0.1% at the maximum displacement (400 μm).

For the spring design shown in Figure 5a, the experimentally determined load-displacement behavior is plotted in Figure 5b, along with the load-displacement curves determined by FEA. Three different thicknesses were modeled (13, 14, and 15 μm), since the actual thickness of the spring was measured to vary between 13 and 15 μm . (The springs were typically thicker near the edges of the frame and the central island, due to the dynamics of the KOH etching.) The FEA predictions match very closely with the experimentally measured behavior, verifying the appropriateness of the FEA technique for this application.

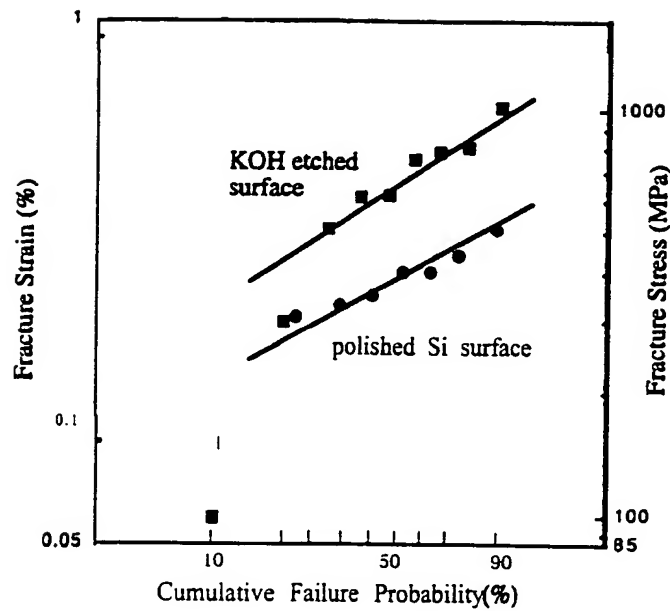


Figure 4. Four point bending test results for silicon bend bars.

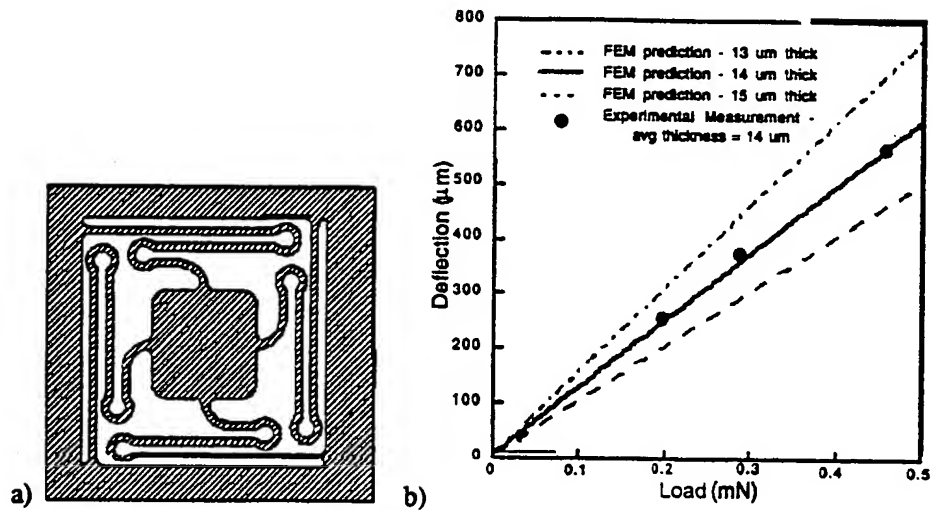


Figure 5. a) Spring design for which the experimental measurements and FEA predictions shown in b) were performed.

From the plot in Figure 5b, however, it is clear that this design will not work for the microvalve application. Though the maximum strain was calculated to be less than 0.05% for 450 μm of deflection, the force applied by the spring is less than 0.5 mN, much less than the 0.1 N which is desired.

Numerous other spring designs were examined, ranging from the straight beam design shown in Figure 6a to the serpentine design shown in Figure 6b. The load-deflection curves for these two spring designs (15 and 20 μm thick, respectively) are plotted in Figure 7. The straight beam design (7a) displays extremely nonlinear behavior, which is inappropriate for this application. In addition, the 0.1% strain limit is exceeded below 50 μm deflection. The serpentine spring (7b) accomplished a large enough deflection with a strain below 0.05%, but the force applied is much too low. From the analyses of the numerous designs it became apparent that very long beams are necessary to achieve large deflections with low strains; however, to attain a high restoring force, the thickness of the beams must increase drastically.

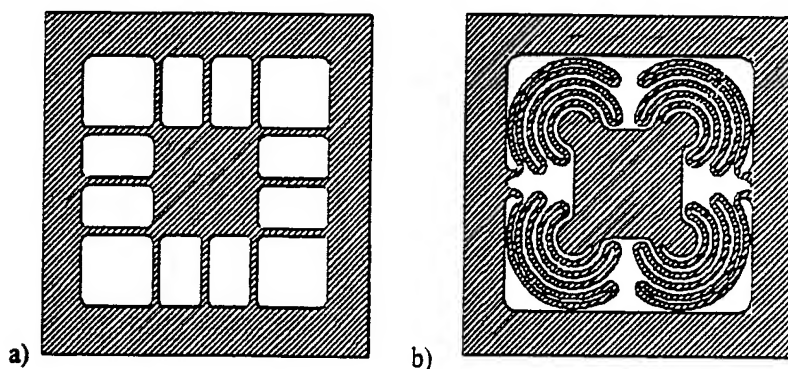


Figure 6. Silicon spring designs with a) straight beams and b) serpentine beams.

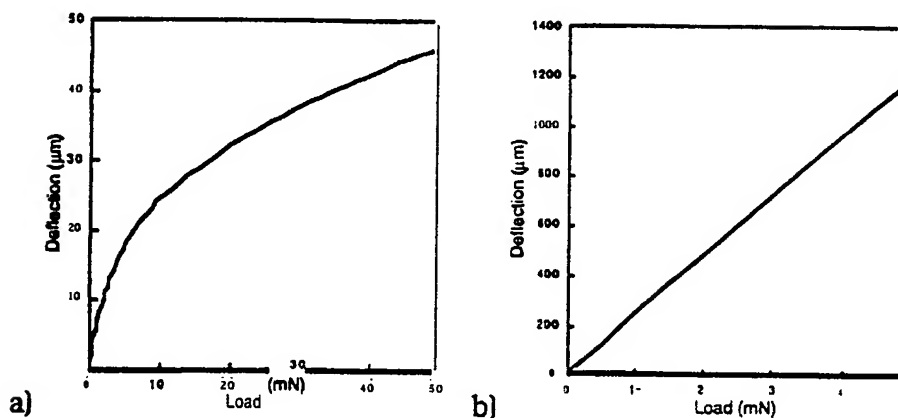


Figure 7. Load/deflection behavior for the spring designs shown in Figure 6.

Recently, etching equipment which utilize novel techniques have become available, which are capable of reactive ion etching through an entire 525 μm thick wafer. Therefore, a new spring design was created which took advantage of this possibility. The design is shown in Figure 8a, with the load-deflection behavior plotted in Figure 8b. A deflection of 150 μm results in a force of 0.1 N, and 400 μm of deflection is achieved below 0.3 N and a strain of 0.08%. Therefore, this spring meets the design criteria for use with the microvalve. Fabrication of these springs has recently been completed.

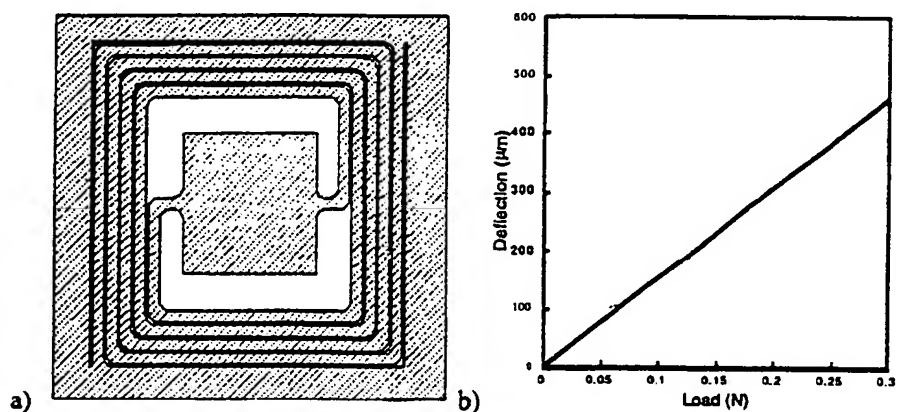


Figure 8. a) New spring design for thick springs; and b) Load/deflection behavior for this spring.

CONCLUSIONS

Silicon microsprings have been designed and fabricated from single crystal silicon wafers, using standard micromachining techniques. Fracture studies showed that the maximum strain which can safely be achieved under operation is 0.1%. Finite element analysis has been experimentally verified to accurately predict the mechanical behavior of the springs. For use in a TiNi shape memory alloy actuated microvalve, FEA has determined that standard silicon processing is not sufficient, because the thickness of the spring required to meet the design specifications is on the order of 500 μm . This can be achieved by novel reactive ion etching techniques.

ACKNOWLEDGMENTS

This work is supported by DARPA under contract no. DABT63-96-C0070. Thick silicon reactive ion etching was performed by Alcatel Comptech, CA.

REFERENCES

- 1 H. Kahn, W.L. Benard, M.A. Huff, and A.H. Heuer, 'Titanium-nickel shape memory thin film actuators for micromachined valves,' MRS Symp. 444, 271 (1997).



MEMS Micropackaging for Microsystems Integration

Sazzadur Chowdhury, G. A. Jullien, M. Ahmadi, W. C. Miller

Research Centre for Integrated Microsystems
Department of Electrical and Computer Engineering
University of Windsor
Windsor, Ontario, N9B 3P4, Canada

Abstract

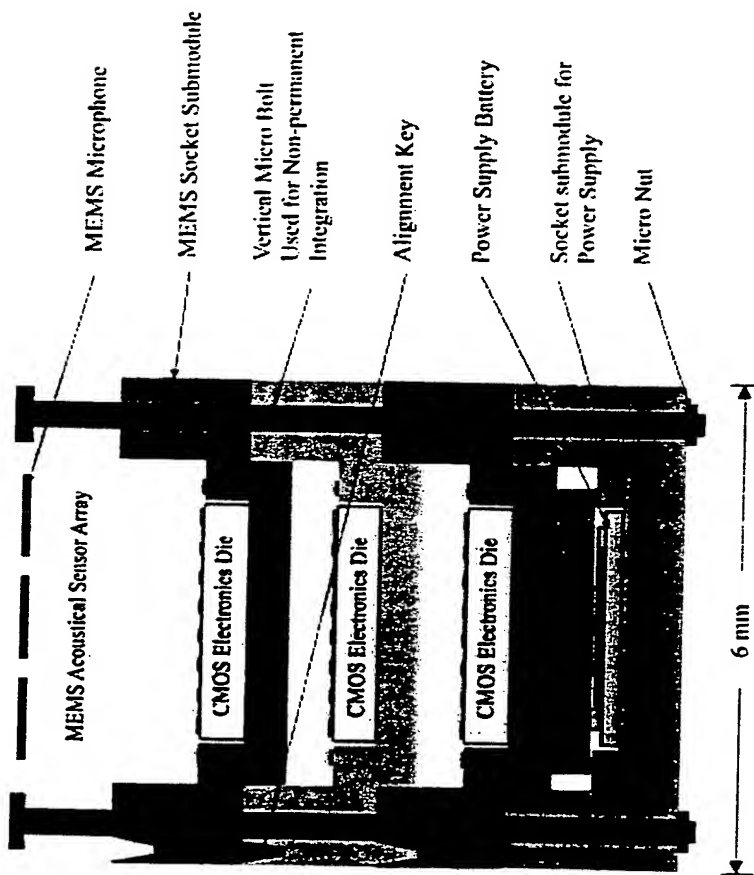
- A modular MEMS socket system has been developed that enables a custom, application-specific micropackaging solution for diverse technology dies and devices
- Each socket submodule may contain a CMOS or non-CMOS die (MEMS, Photonics, RF, GaAs, BJT, etc.) or may itself be a sensor/actuator or microanalyzer
- An insertable/removable MEMS microbus card provides connectivity among socket submodules and slides into an interconnection channel prefabricated in all submodules
- The system can also be configured for testing of high density I/O SoC dies or diverse-technology systems using a solderless, pressure dependent cantilevered bridge-type microspring contact mechanism



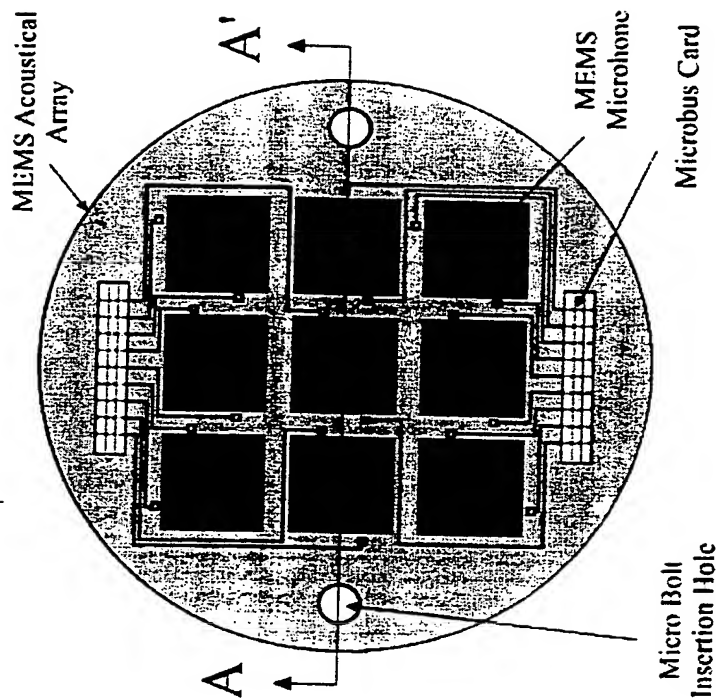
MEMS Micropackaging Solution: Major Design Features

- A complete working system in a package offering diverse micropackaging solutions
- Scalable single or modular micropackaging
- Permanent or temporary submodule integration
- Socket submodules to accommodate integrated circuit dies in custom fabricated housing pits
- A sensor can itself be a socket submodule or can be surface mounted in a socket submodule
- An insertable/removable microbus card provides custom inter-modular connectivity
- Heat deformed, gold coated cantilever microsprings on the microbus card connects to platinum coated microrail contacts inside the vertical interconnection channel in a submodule
- Gold wire bonding between Socket metal pads and die I/O pads
- Low impedance connectivity path
- Conduction type thermal management
- Cantilevered bridge-type microspring contact enables dies testing
- Easily modifiable connectivity using microbus card
- Batch fabrication using MEMS technology

Illustration of Modular Integration of a MEMS Sensor and SoC Dies



Section A-A'



Top View

BEST AVAILABLE COPY



Illustration of Microbus Card Connectivity for Various Submodules

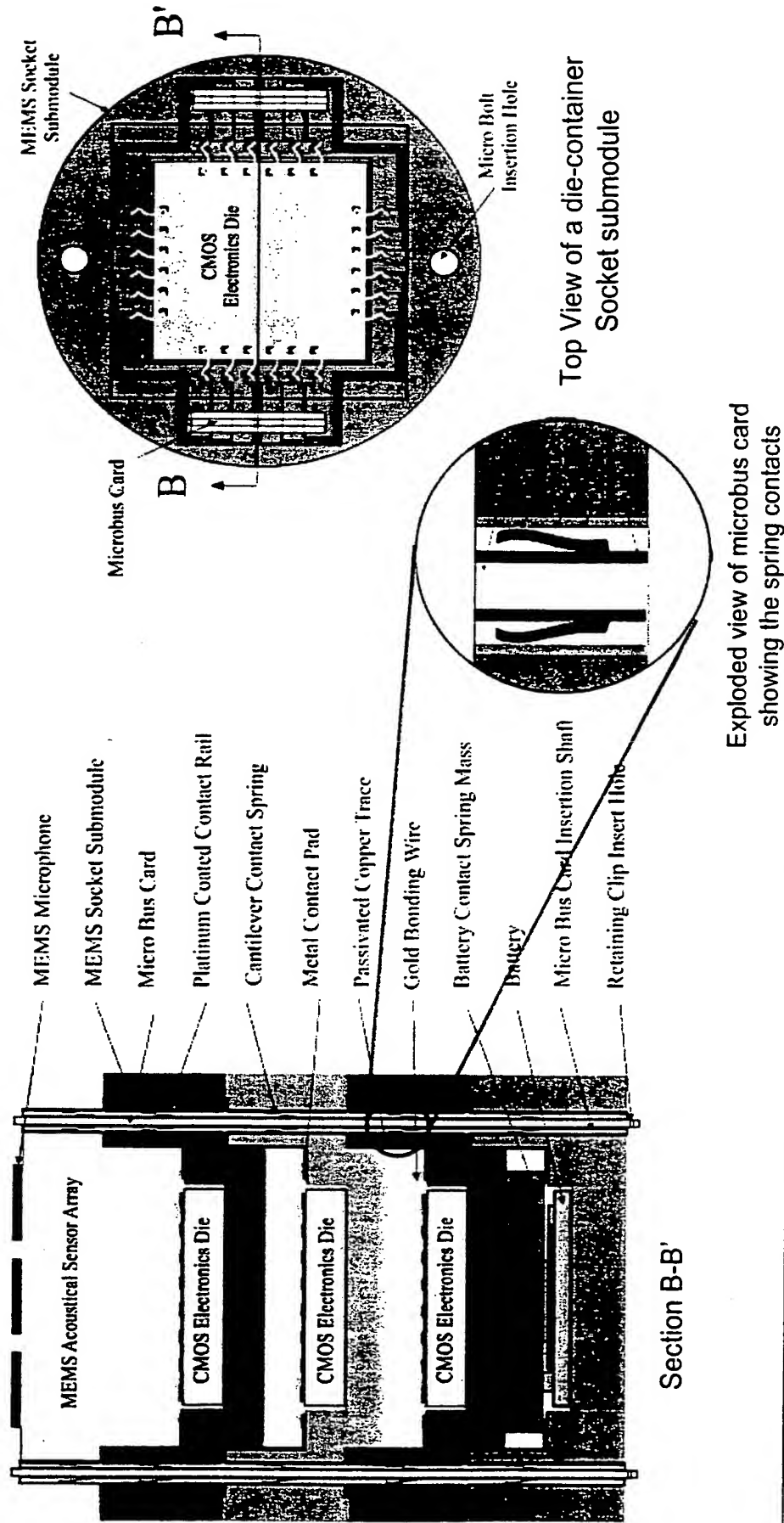
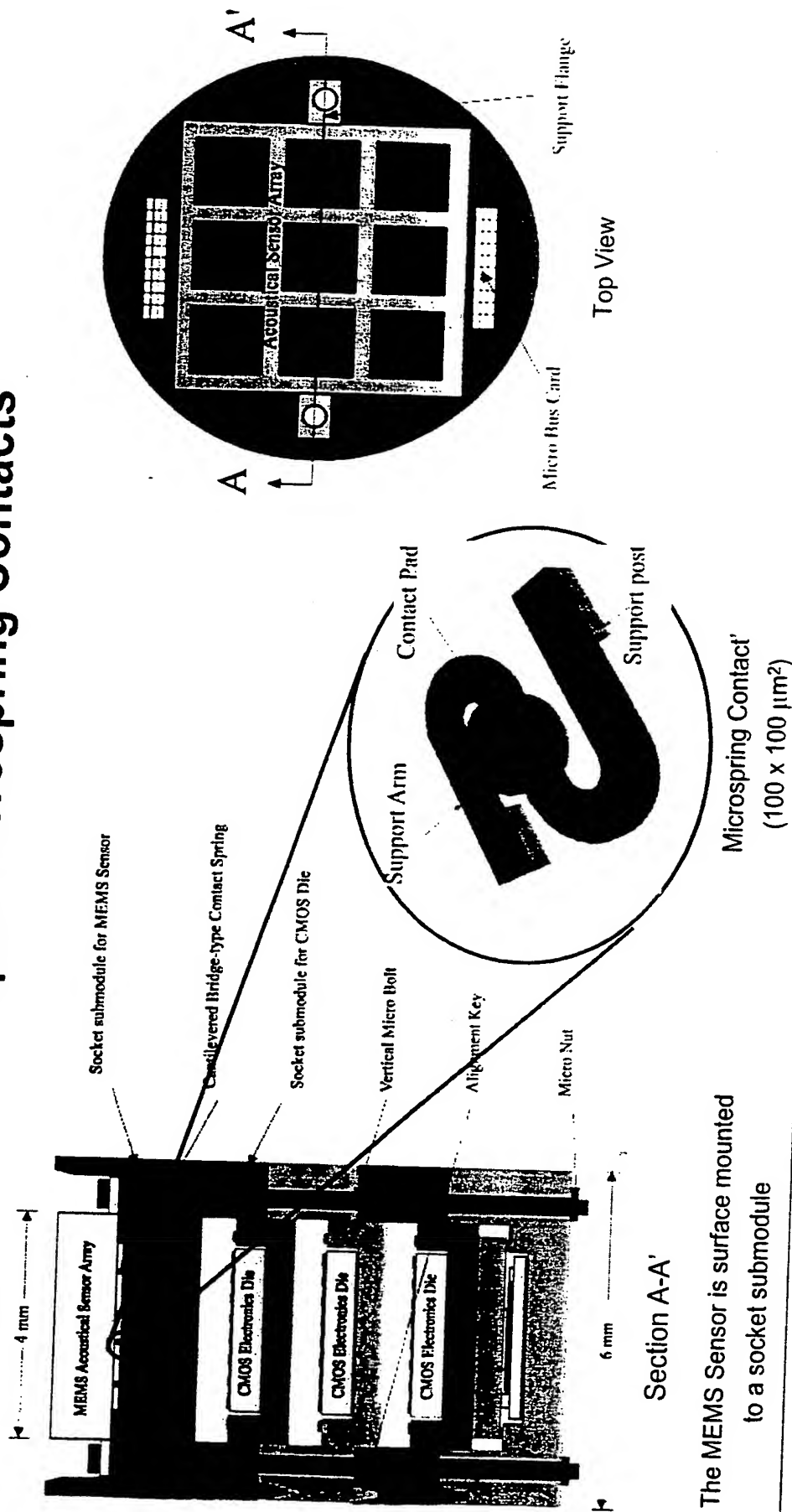


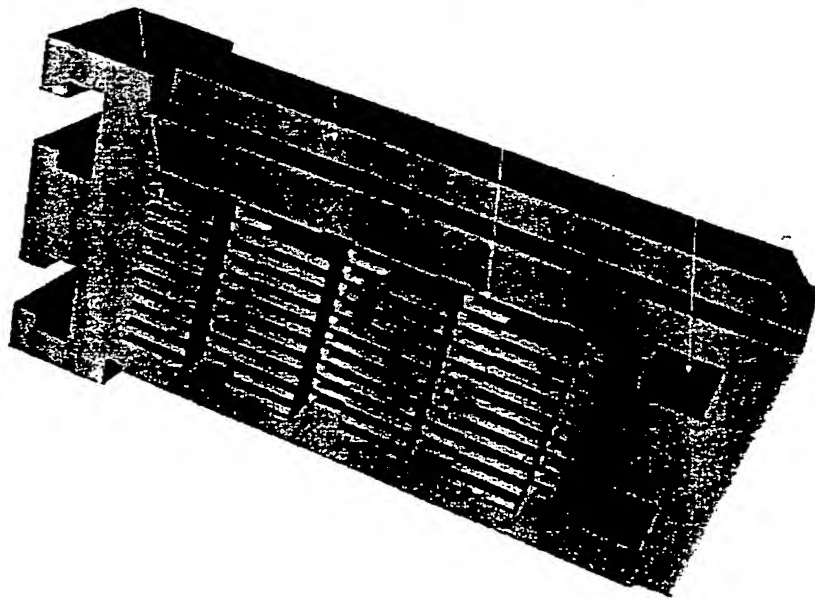


Illustration of Temporary Connectivity Using Z-Shaped Microspring Contacts





Microbus Card Connectivity System



Polysilicon
cantilever
Spring

Alignment
Key

Aluminum
Bus

Retaining Clip
Insert Hole

- The microbus card establishes Inter-module connectivity when shoved in through an interconnection channel that is present in each socket submodule
- The microbus card is fabricated using MEMS technology
- The gold coated polysilicon cantilevers are heat treated after fabrication at 150-200° C to induce tensile stress so that the cantilevers bend upwards
- When shoved in, the bent cantilevers come in contact with vertical platinum coated microrails inside the interconnection channel and undergo deformation to generate necessary contact force
- Polysilicon Cantilever Dimensions: 100 x 25 x 2 μm
- Gold Conductor Thickness: 200 nm
- Aluminum Bus Dimensions (W/T): 25 x 1 μm
- Retaining Clip Insertion Hole (L/W): 250 x 250 μm
- Microbus Card Dimensions (W/T): 2 mm x 400 μm
- Microbus card Material: Czochralski Silicon

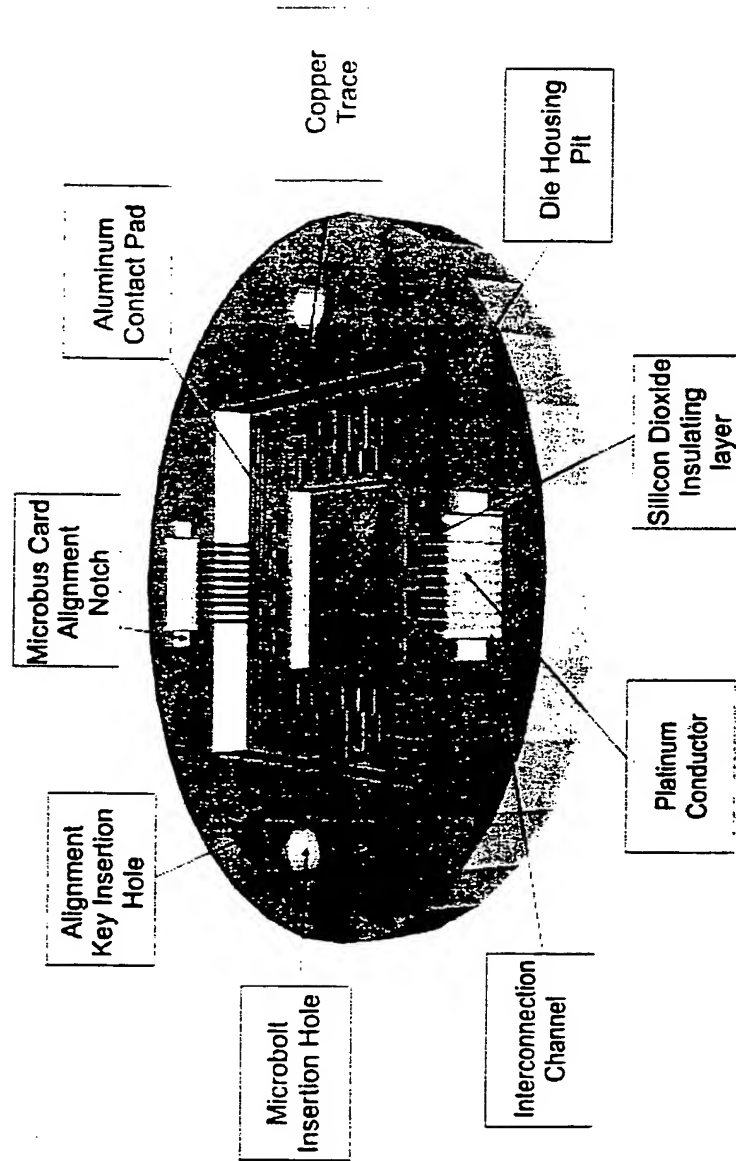
Microbus Card 3-D model Before Heat Treatment. Generated by IntelliSuite Design Tools Simulating Fabrication Processes

Major Design Specifications



MEMS Socket: Die Container Submodule

3-D model of a die container type MEMS socket submodule after simulating the fabrication processes using IntelliSuite design tools

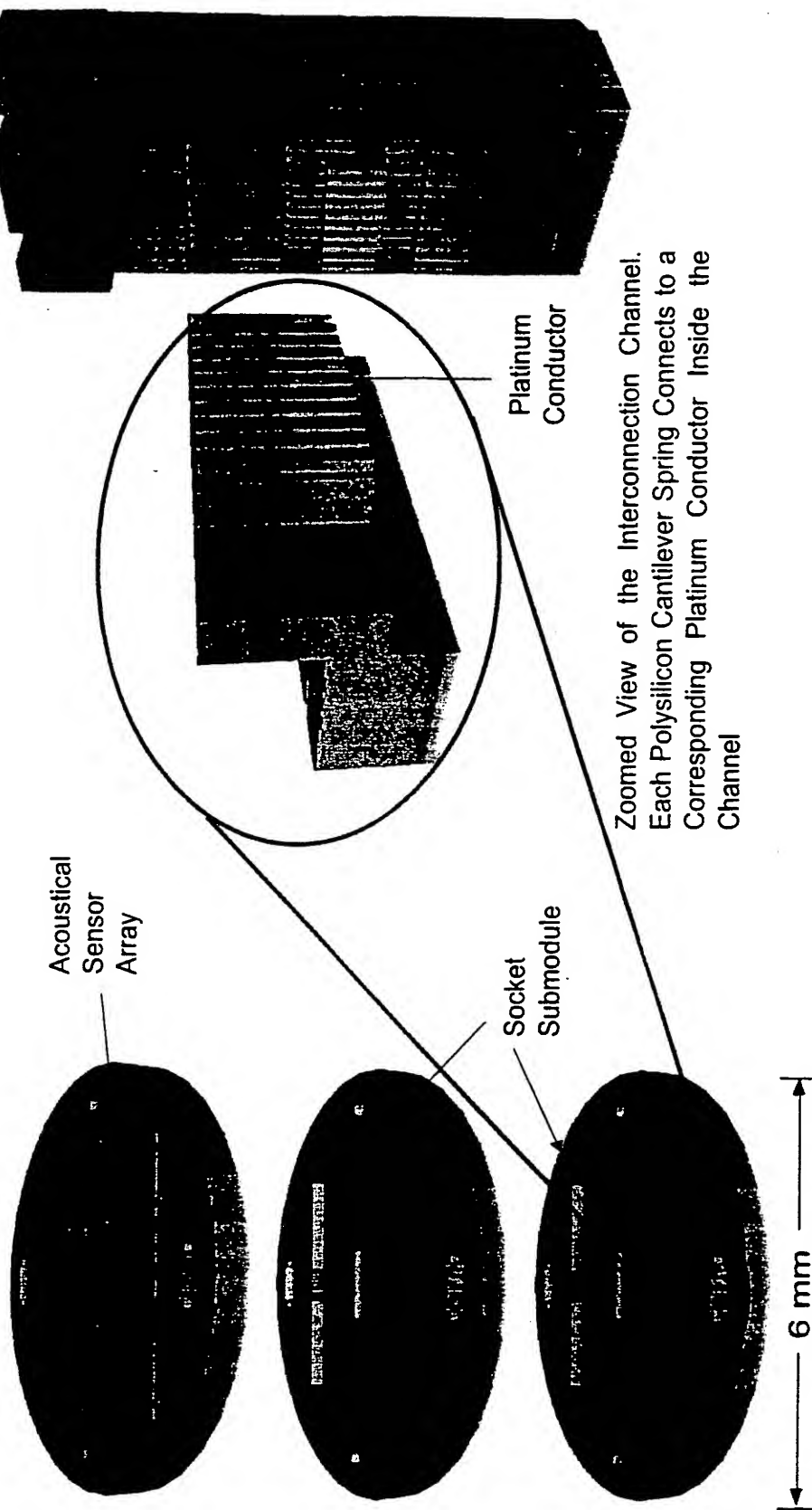


Major Design Specifications

- Socket Submodule Thickness : 400 μm
- Depth of CMOS Die Insertion Pit: 100 μm
- Thickness of Backside Extrusion: 100 μm
- Microrail Dimensions (W/H): 25/200 μm
- Metal Contact Pad Area: 75 x 75 μm
- Micro Bolt Diameter: 400 μm
- Interconnection Channel
- Dimensions (W/T): 2 mm/400 μm
- Platinum Conductor Thickness: 200 nm

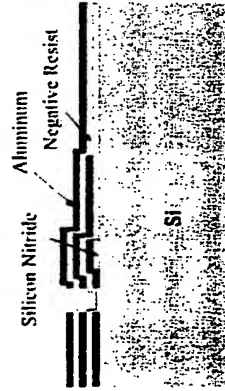


Micropackaging Example: Integration of an Acoustical Sensor Array with a SoC

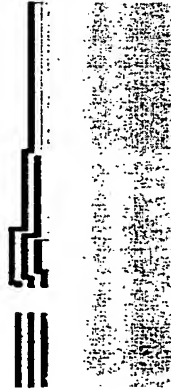




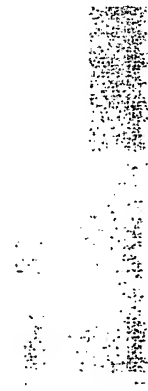
MEMS Socket Submodule Fabrication Process



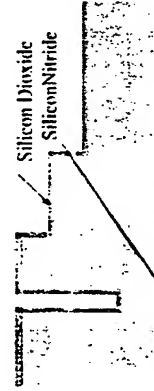
70 nm thick PECVD silicon nitride is deposited, patterned and etched on the top of a 400 μm thick silicon wafer. Three layers of aluminum-negative photoresist laminations are deposited.



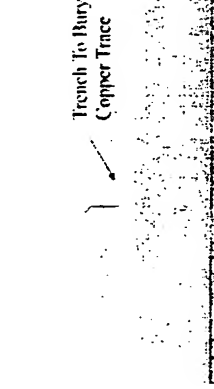
O_2 ashing of the negative photoresist is carried out by ICP-RIE method. The wafer is then successively ICP-RIE etched using Aluminum and negative resist laminations as delayed mask.



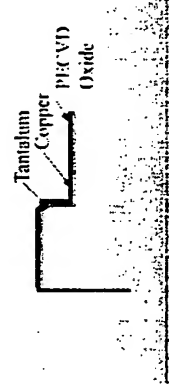
After the 3rd ICP-RIE process, the wafer patterning is completed. The 3rd Aluminum mask is then stripped.



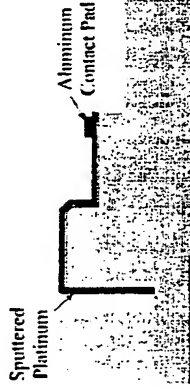
70 nm thick PECVD nitride is then deposited and patterned on the wafer backside. Thermal oxide is grown on both sides of the wafer and patterned.



PECVD nitride on the wafer topside is removed. The wafer is TMAH etched to form the slant corner on the top. The wafer is then RIE etched to form 5 μm deep by 35 μm wide trenches.



Tantalum is sputter deposited and patterned in the trenches. 1.0 μm thick copper is sputtered and patterned. Finally a 3.5 μm thick silicon dioxide is PECVD deposited to protect the copper traces from oxidation.



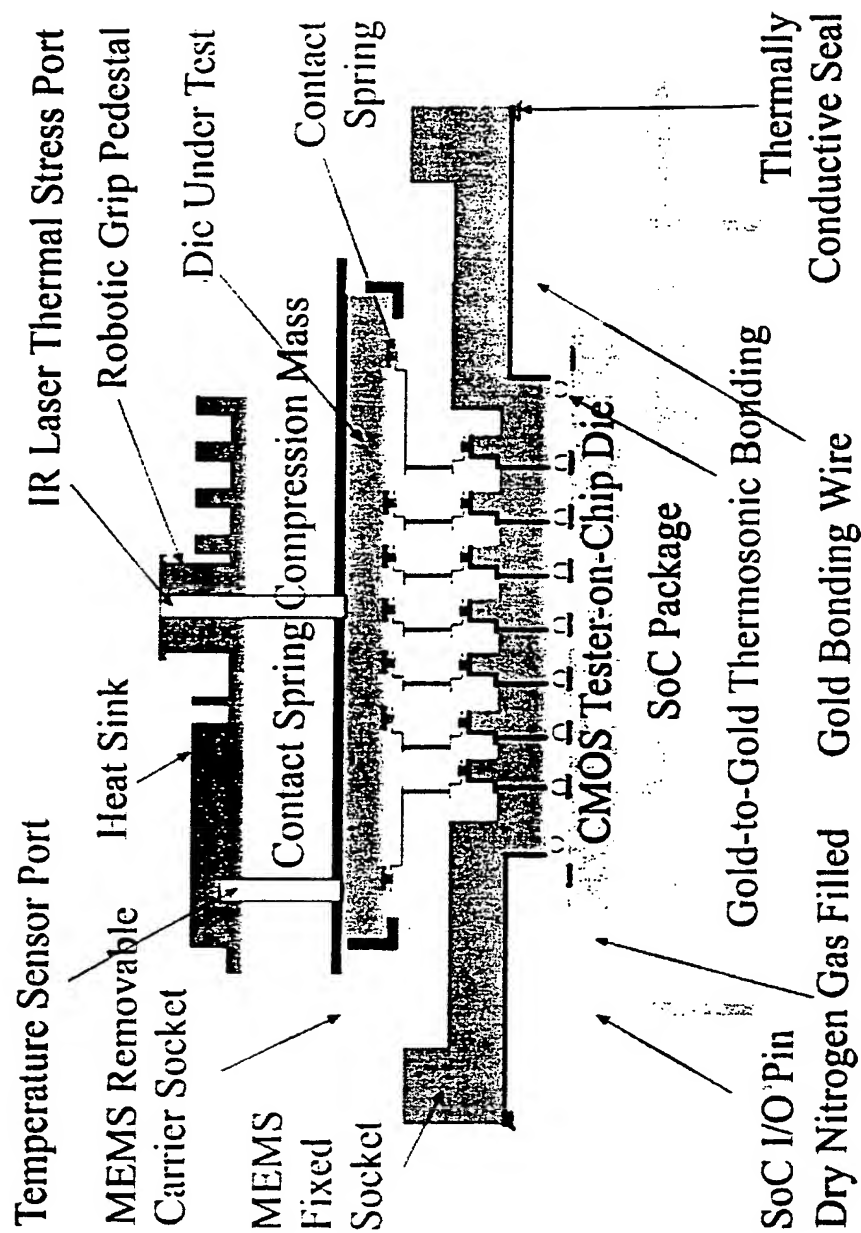
75x75 μm^2 Aluminum contact pads are then formed. 200 nm thick platinum is then sputter deposited in the interconnection shaft and patterned using an electrodeposited photoresist.



Wafer backside nitride is stripped. Anisotropic etching is performed on the wafer backside using TMAH to complete the fabrication process.

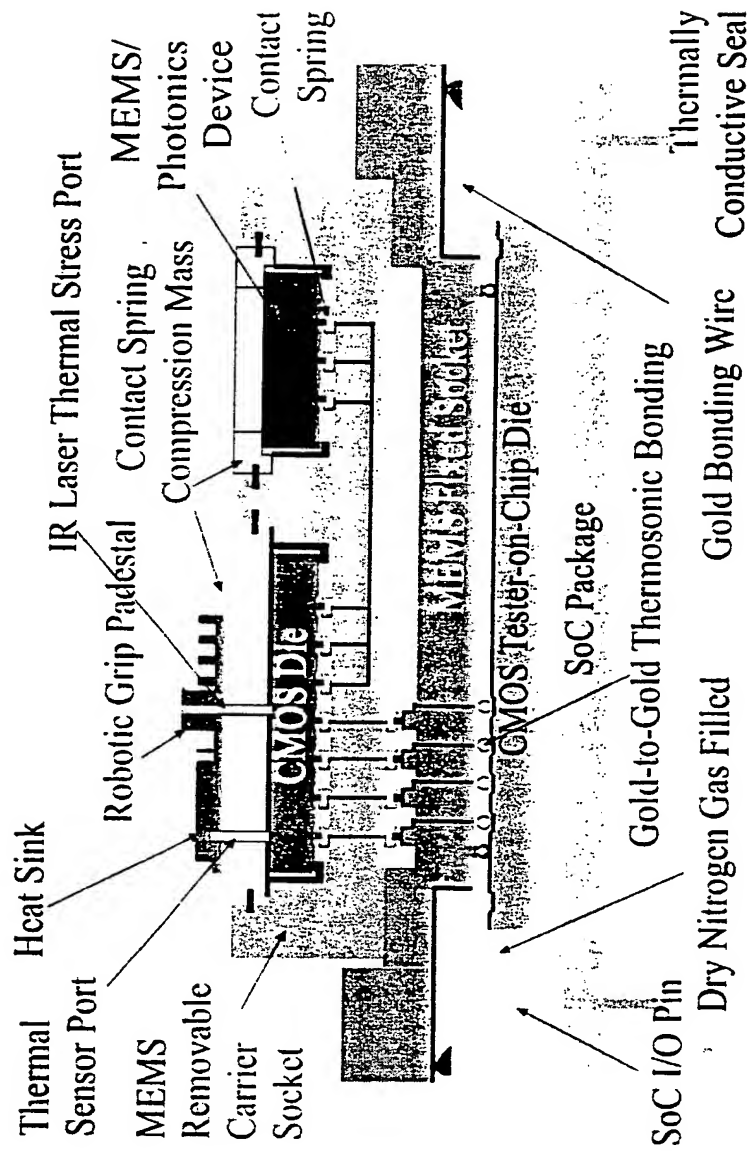


CMOS Die Testing Configuration: Concept





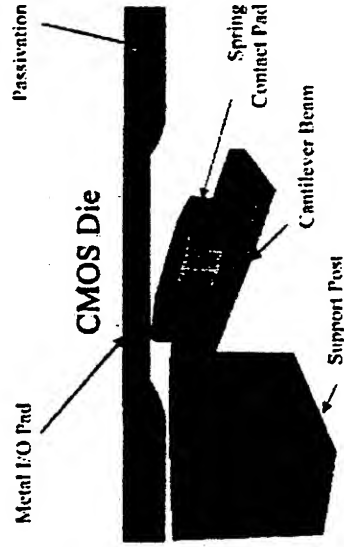
Multiple Technology Devices or Systems Testing Configuration





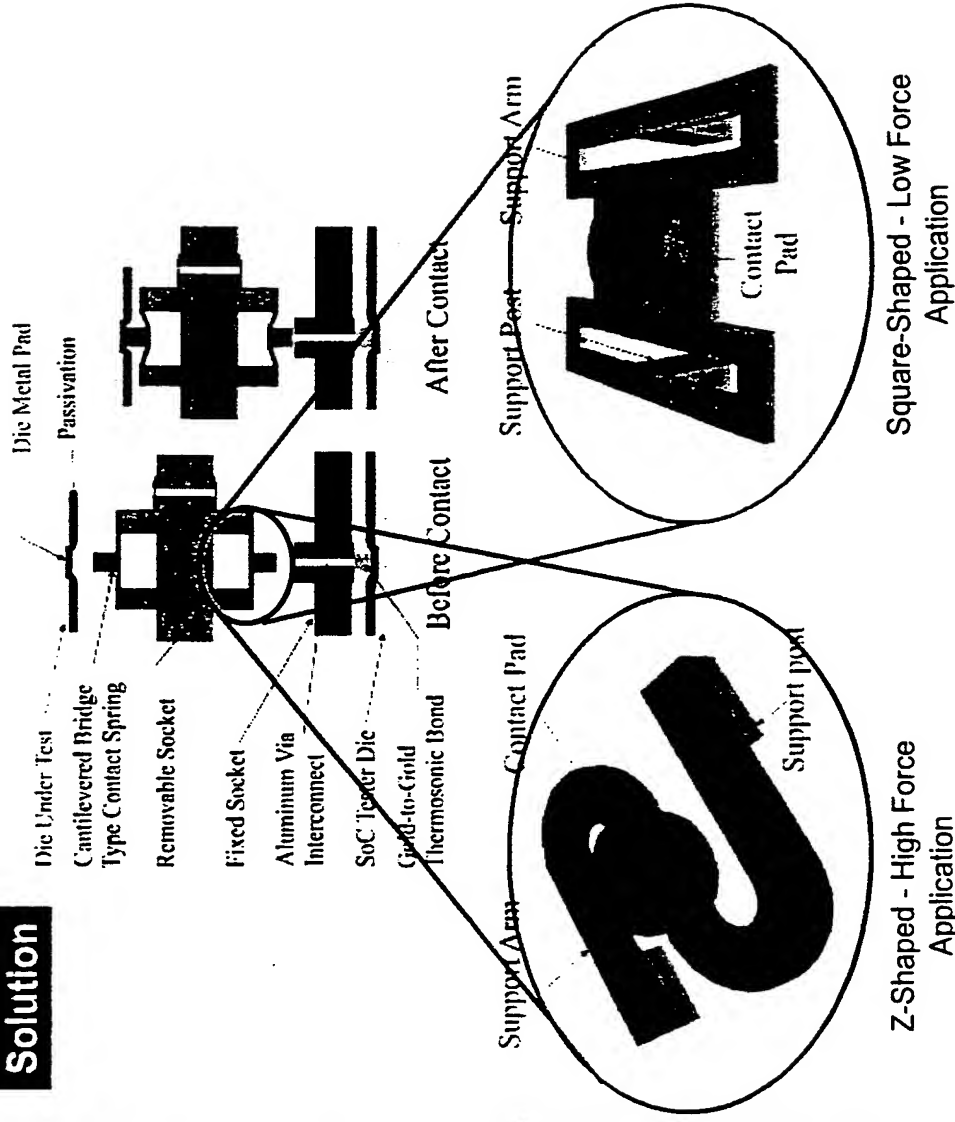
Microspring Contact Design Considerations

Problem



- Due to a uniform pressure applied on the top, the contact pad undergoes a torsional deformation that results in a curved top surface
- The whole contact pad surface does not come in contact with the die metal pad
- The result is a higher resistance line-type (arc) contact

Solution





Microspring Contact Design specifications

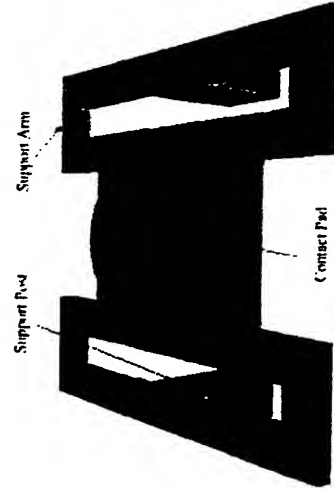


Z-shaped Geometry

- Spring area: $100 \times 100 \mu\text{m}^2$
- Contact pad diameter: $40 \mu\text{m}$
- Contact pad height: $10 \mu\text{m}$
- Support arm thickness: $5 \mu\text{m}$
- Support arm width: $20 \mu\text{m}$
- Contact force: 5 mN
- Spring material: Copper

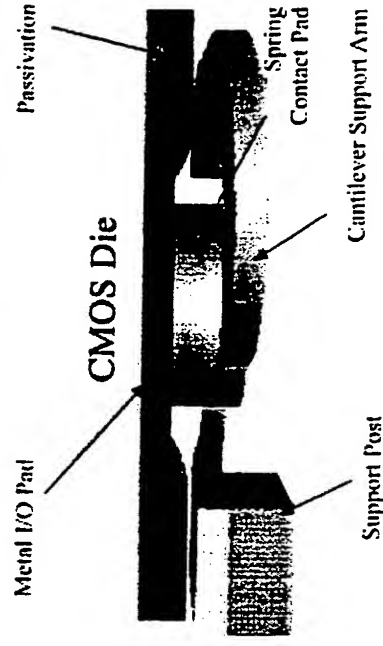
Major Design Features

- $150 \mu\text{m}$ pitch
- $30 \mu\text{m}$ tolerance in both X and Y directions
- Excellent elastic properties
- $19.3 \text{ m}\Omega$ contact resistance
- Excellent thermal properties at 150°C
- Further down scalable



Square Geometry

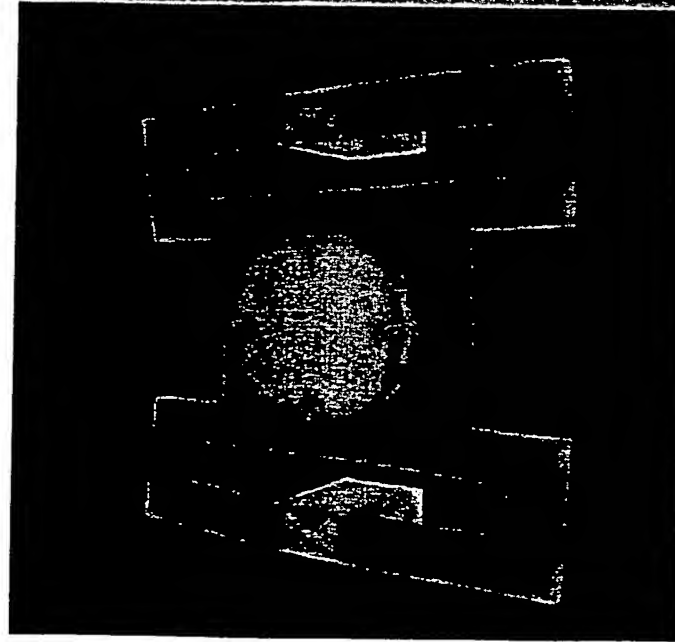
- Spring area: $100 \times 100 \mu\text{m}^2$
- Contact pad diameter: $40 \mu\text{m}$
- Contact pad height: $5 \mu\text{m}$
- Support arm thickness: $2 \mu\text{m}$
- Support arm length: $70 \mu\text{m}$
- Contact force: 1.35 mN
- Spring material: Copper



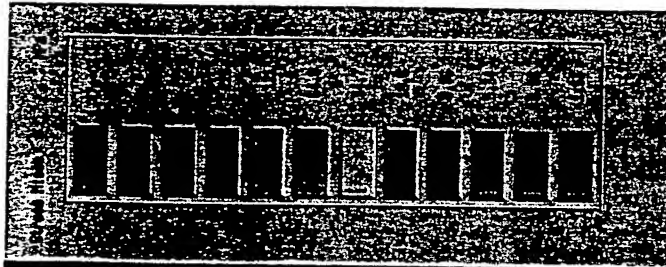
Result: Excellent Connectivity



FEA Simulation Results: Square-Shaped Microspring Contact



Von Mises stress (Max. 1.47 GPa)

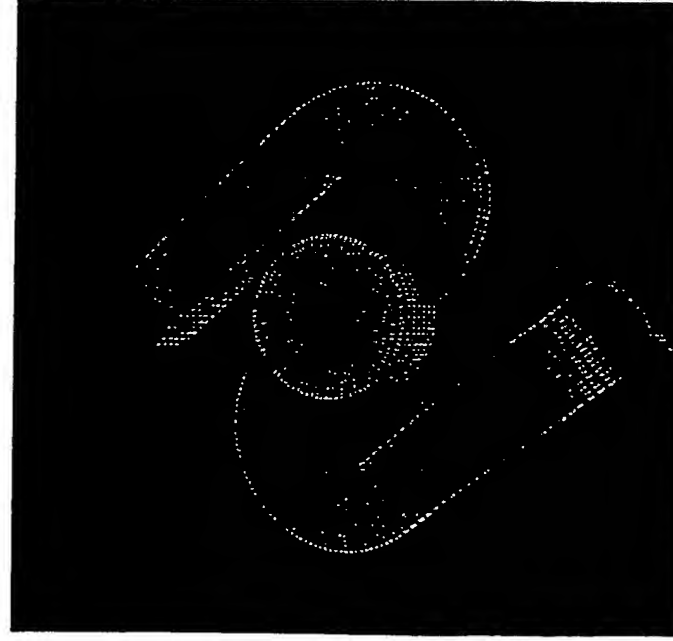


Z-axis displacement is uniform throughout the contact pad area

The Von Mises stress is within the elastic limit of copper with a reasonable safety margin for the desired Z-axis displacement
Applied force: 1.35 mN
Max. Z-axis displacement: 5 μm

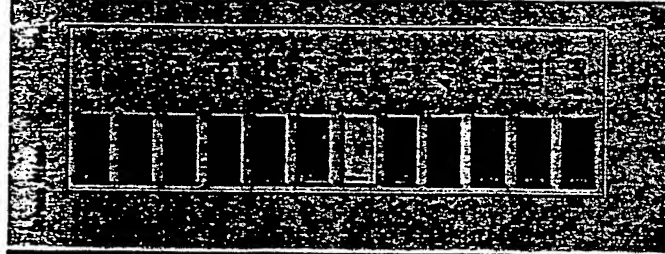


FEA Simulation Results: Z-shaped Microspring Contact

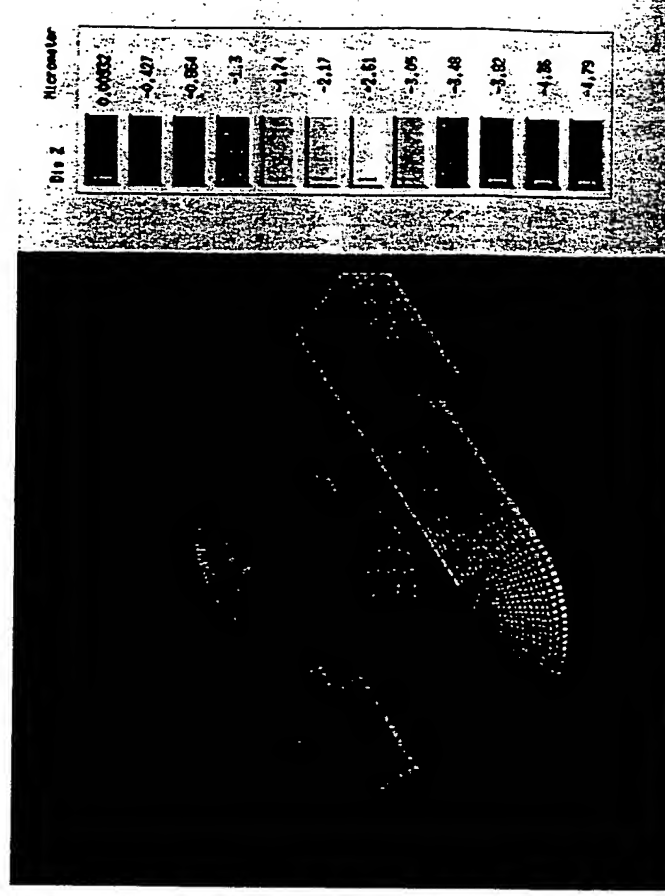


Von Mises stress (Max. 1.46 GPa)

The Von Mises stress is within the elastic limit of copper with a reasonable safety margin for the desired Z-axis displacement
Applied force: 5 mN
Max. Z-axis displacement: 4.8 μm



Z-axis displacement is uniform throughout the contact pad area





Conclusions

The design of a MEMS micropackaging system is presented that enables SoC integration. Major components of the system consist of MEMS socket submodules and insertable/removable microbus card(s). The system demonstrates advantages over conventional packaging systems in terms of: (a) easy removal or integration of a new die/device; (b) permanent or non-permanent module integration; (c) reconfigurable connectivity using microbus card, and; (d) an application specific custom packaging geometry that can be batch fabricated using MEMS technology.

Acknowledgements

The research has been made possible by the interest and support provided by the Gennum Corporation of Burlington, Ontario. The authors greatly acknowledge the generous support of the following partners: CMC, MICRONET and NSERC. The Research Centre for Integrated Microsystems at the University of Windsor would like to acknowledge the access to the outstanding MEMS technology provided by the IntelliSense Corporation, 16 Upton Drive, Wilmington, MA 01887, USA as part of a collaborative partnership.

References

1. Yoshio Mita, Makoto Mita, Agnes Tixier, Jean-Phillipe Gouy and Hiroyuki Fujita, "Embedded-Mask-methods for mm-scale Multilayer Vertical/Slanted Si Structures", *Proceedings of MEMS 2000 Conf.*, Miyajaki, Japan, pp. 300-305.
2. Agnes Tixier, Yoshio Mita, Satoshi Oshima, Jean-Phillipe Gouy and Hiroyuki Fujita, "3-D Microsystem Packaging for Interconnecting Electrical, Optical and Mechanical Microdevices to the External World", *Proc. of MEMS 2000 Conf.*, Miyajaki, Japan, pp. 698-703.
3. H. Goldstein, "Packages Go Vertical", *IEEE Spectrum*, August 2001, pp. 46-51.